

# Adaptive Layer Selection for Efficient Vision Transformer Fine-Tuning

Alessio Devoto<sup>1,3</sup> Federico Alvetreti<sup>1</sup> Jary Pomponi<sup>1,3</sup>  
Paolo Di Lorenzo<sup>1,3</sup> Pasquale Minervini<sup>2</sup> Simone Scardapane<sup>1,3</sup>

<sup>1</sup> La Sapienza, University of Rome

<sup>2</sup> The University of Edinburgh <sup>3</sup> CNIT

<sup>1</sup> {firstname.lastname}@uniroma1.it <sup>2</sup> p.minervini@ed.ac.uk

## Abstract

Recently, foundation models based on Vision Transformers (ViTs) have become widely available. However, their fine-tuning process is highly resource-intensive, and it hinders their adoption in several edge or low-energy applications. To this end, in this paper we introduce an efficient fine-tuning method for ViTs called **ALaST** (*Adaptive Layer Selection Fine-Tuning for Vision Transformers*) to speed up the fine-tuning process while reducing computational cost, memory load, and training time. Our approach is based on the observation that not all layers are equally critical during fine-tuning, and their importance varies depending on the current mini-batch. Therefore, at each fine-tuning step, we adaptively estimate the importance of all layers and we assign what we call “compute budgets” accordingly. Layers that were allocated lower budgets are either trained with a reduced number of input tokens or kept frozen. Freezing a layer reduces the computational cost and memory usage by preventing updates to its weights, while discarding tokens removes redundant data, speeding up processing and reducing memory requirements. We show that this adaptive compute allocation enables a nearly-optimal schedule for distributing computational resources across layers, resulting in substantial reductions in training time (up to 1.5x), FLOPs (up to 2x), and memory load (up to 2x) compared to traditional full fine-tuning approaches. Additionally, it can be successfully combined with other parameter-efficient fine-tuning methods, such as LoRA.

## 1 Introduction

Recently, large-scale Vision Transformers (ViTs, (Dosovitskiy et al. 2021)) have become the leading paradigm in computer vision. By leveraging the self-attention mechanism, ViTs can capture long-range dependencies in images at every layer, leading to superior results compared to traditional convolutional neural networks (CNNs). ViTs are at the core of a wide array of applications, ranging from vision-language models (Radford et al. 2021; Matthias Minderer 2022; Liu et al. 2023) to resource-constrained embedded devices (Cai, Gan, and Han 2022; Cai et al. 2020; Mehta and Rastegari 2022; Laskaridis et al. 2020).

The impressive capabilities of ViTs come with the drawback of a resource-intensive training process. The high computational demands arise from the large number of parameters and the quadratic complexity of the self-attention mechanism. Moreover, ViTs are extremely data-hungry, requiring

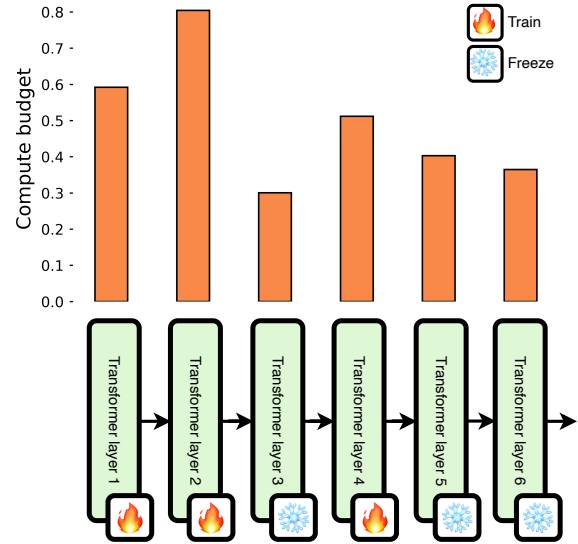


Figure 1: At each fine-tuning step, we assign what we call “compute budgets” to transformer layers. The budget determines the computational resources we invest in each layer, i.e., (a) whether the layer is frozen or trainable and (b) how many tokens that layer can process. By adaptively allocating the budget, we make the fine-tuning faster and more efficient in terms of FLOPs, memory, and time.

large datasets to achieve optimal performance, which in turn prolongs training times.

To address these constraints, a common practice for the deployment of ViTs is to leverage a pre-trained foundation model and then perform fine-tuning for specific tasks. By updating only a subset of the model parameters, fine-tuning makes it feasible to achieve high performance on specialized tasks without the prohibitive costs associated with training a model from scratch (Xin et al. 2024). However, fine-tuning ViTs introduces additional complexity: the choice of which parameters to update is critical, as it can significantly impact performance (Sarkar et al. 2024). Identifying the optimal layers to fine-tune often requires extensive experimentation, which is not always feasible in real-world scenarios due to time and computational constraints. Parameter-efficient

fine-tuning (PEFT) methods, such LoRA (Hu et al. 2022) or adapters (Houlsby et al. 2019) aim to address some of these challenges, but they often focus on optimizing the count of additional parameters rather than reducing overall computational load. As a result, PEFT methods might still be unsuitable for highly constrained environments where minimizing computation and memory are limited (Sarkar et al. 2024). This is the case for mobile and edge devices, drones or next-generation 6G networks that face strict constraints on memory and computational resources (Cai, Gan, and Han 2022; Cai et al. 2020; Calvanese Strinati et al. 2024). These devices require lightweight models that can be quickly fine-tuned on a low budget without compromising performance. Similarly, in situations where privacy concerns prevent data from being sent to a server, on-device processing and fine-tuning become essential.

In this work, we propose a simple method to accelerate the fine-tuning of ViTs in low-resource settings by leveraging two key insights. First, it is known that not all *tokens* are equally useful during training, due to redundant information present in input images. Various techniques have been developed to estimate token importance and either discard, merge, or halt redundant tokens to enhance *inference* (not training) speed, showing promising results (Meng et al. 2022; Bolya et al. 2023; Rao et al. 2021). Second, not all *layers* are equally important during training. Some layers receive minimal updates due to small gradients, making associated computation inefficient in both the forward and backward pass. Building on these observations, we propose *Adaptive Layer Selective fine-Tuning for Vision Transformers* (ALaST) — during fine-tuning, we allocate a so-called scalar *budget* to each layer, and we control resource consumption along two axes: the number of discarded tokens and the selection of trainable layers. Specifically, we *adaptively* determine (a) how many tokens to forward through each layer and (b) which layers to freeze based on the budget allocation. Discarding tokens significantly reduces FLOPs — due to the quadratic cost of multi-head attention — and accelerates training, especially on mid-range GPUs, enabling models to reach higher accuracy in shorter time. Freezing layers enhances energy efficiency and substantially reduces memory usage, which is critical for on-device training.

We are the first, to the best of our knowledge, to introduce an adaptive framework that systematically optimizes both token and layer selection during fine-tuning, addressing the computational challenges of ViTs in resource-constrained environments. We validate our method against a comprehensive set of baseline approaches, ensuring that our results are robust and demonstrating that ALaST achieves superior efficiency while maintaining competitive accuracy.

## 2 Background on Vision Transformer

A Vision Transformer (ViT) processes an image  $X \in \mathcal{R}^{C \times H \times W}$  (where  $C, H, W$  are channels, width, and height respectively) through a series of  $L$  transformer layers. The transformation pipeline can be formalized as follows:

$$y = \mathcal{C} \circ \mathcal{F}^L \circ \mathcal{F}^{L-1} \circ \dots \circ \mathcal{F}^1 \circ \mathcal{E}(X), \quad (1)$$

where  $\mathcal{E}(\cdot)$  denotes the encoding network,  $\mathcal{F}^i$  represents the  $i$ -th transformer layer, and  $\mathcal{C}(\cdot)$  is the classification head. The encoding network  $\mathcal{E}(\cdot)$  splits the image into smaller, non-overlapping patches. Each patch is then flattened and linearly projected into a lower-dimensional embedding space, forming tokens. Suppose the image is divided into  $N$  patches, each of size  $P \times P$ , resulting in a sequence of  $N$  tokens. This can be represented as:

$$\mathcal{E}(X) = [t_1, t_2, \dots, t_N], \quad (2)$$

where  $t_i \in \mathcal{R}^E$  is the embedding of the  $i$ -th patch, and  $E$  is the embedding dimension. To enable classification, a special trainable token, known as the *class token* (CLS token), is prepended to the sequence of patch embeddings. Additionally, since transformers lack an inherent sense of order, positional encodings are added to each token to retain spatial information. The transformer layers  $\mathcal{F}(\cdot)$  process this sequence of tokens through a series of operations involving multi-head self-attention and feed-forward neural networks. A generic transformer block at layer  $l$  transforms each token from layer  $l - 1$  via:

$$t_l = \mathcal{F}^l(t_{l-1}), \quad (3)$$

where  $t_{l-1}$  denotes the token embedding at layer  $l - 1$ ,  $t_l$  the updated token embedding, and  $\mathcal{F}$  represents a standard transformer encoder block with multi-head attention and a feed-forward MLP. The self-attention operation has a quadratic complexity with respect to the sequence length, i.e. it has a cost of  $\mathcal{O}(N^2)$ , where  $N$  is the number of tokens. This quadratic cost can be significant for devices with limited resources. Efficient implementation techniques or approximations are often required to make ViTs faster and more memory efficient for inference on downstream tasks, especially in low resource settings (Meng et al. 2022; Yin et al. 2022; Bolya et al. 2023).

The CLS token, which aggregates information from all patches, is extracted after the final transformer layer and passed to the classification head  $\mathcal{C}(\cdot)$ . This head typically consists of a linear layer followed by a softmax function to produce the final classification output. We show an overview of the Vision Transformer architecture adapted to our method in Figure 3.

### 2.1 Layer Contributions during Fine-tuning

We analyze the transformer architecture from the perspective of the residual stream, as described by Elhage et al. (2021). In this framework, the set of tokens flows through the model, with token embeddings being updated via vector additions from the attention and feed-forward blocks in each layer. This perspective allows us to isolate and examine the individual contributions that each layer adds to the residual stream.

Multiple studies (Samragh et al. 2023; Zhang, Bengio, and Singer 2022; Gromov et al. 2024) have demonstrated that not all layers contribute equally to the updates in the residual stream. This phenomenon is particularly evident in pre-trained models, where some layers function almost like identity mappings, providing minimal updates to the token embeddings in the residual stream.

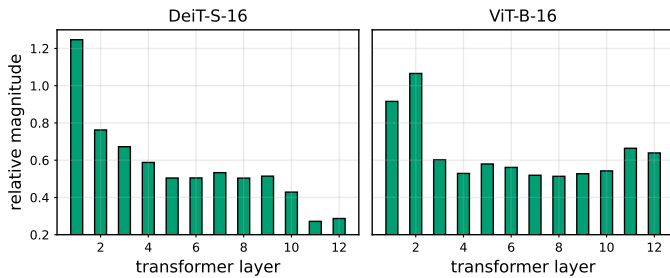


Figure 2: Relative magnitude  $\frac{|f(x)|}{|f(x)+x|}$  for each transformer layer in pre-trained DeiT-S (left) and ViT-B (right). Layers with low relative magnitudes (final ones for DeiT-S and middle ones for ViT-B) provide a minimal contribution to the residual token stream, working as identity functions.

To visually illustrate this behavior, we define the relative magnitude of a transformer layer as the ratio of the non-residual block’s contribution to the overall layer output. Specifically, given the layer input  $x$  and the layer’s contribution  $f(x)$ , we follow Samragh et al. (2023) and plot the relative magnitude  $\frac{|f(x)|}{|f(x)+x|}$  for each transformer layer. Small values indicate that the layer is leaving the input largely unchanged. We present an example of this for ViT-B and DeiT-S in Figure 2.

From an efficiency standpoint, performing computations in layers that do not significantly alter the input embeddings is a waste of computational resources, especially when those layers are being trained. This insight has been applied in various ways, such as distilling large language models into smaller ones (Gromov et al. 2024) or initializing smaller transformers for fine-tuning (Samragh et al. 2023). More recently, Sarkar et al. (2024) identified the most important layers in a ViT and focused on fine-tuning only those layers. While these strategies produce competitive results, they come with the drawback of requiring extensive experimentation to identify the optimal combination of layers to train. In contrast, we introduce a method that automatically learns which layers are most important, eliminating the need for such experimentation.

### 3 Adaptive Layer Selective Fine-tuning

Because different layers affect the final prediction in different ways (Dodge et al. 2020; Samragh et al. 2023), pre-determining which layers to fine-tune can result in sub-optimal outcomes. Previous approaches have attempted to identify the most critical layers through extensive search methods (Samragh et al. 2023; Sarkar et al. 2024; Gromov et al. 2024). However, these methods are highly dependent on the specific dataset and model being used, leading to inconsistencies when applied to different data distributions or model scales. For example, an exhaustive search might determine that layers 4, 5, and 6 are the most important when fine-tuning on the Flower-102 dataset, leading to the decision to freeze the other layers. Yet, this configuration may not be effective for a different dataset, necessitating another round of exhaustive searching. Similarly, the important lay-

ers in ViT-B may differ from those in DeiT-T, requiring a separate search for each model.

To overcome these challenges, we propose a simple strategy that *adaptively* estimates the importance of each layer during fine-tuning, leading to improvements in memory usage, FLOPs, and wall-clock training time. This approach is especially valuable in low-resource scenarios, where it can be integrated requiring minimal modifications to existing training pipelines. In such scenarios where resources are limited, we argue that not all layers should be trained with the same computational effort; some layers should receive a reduced computational budget and therefore be trained with fewer resources.

To optimize resource allocation, we focus on two key parameters: the number of tokens processed by each layer and which layers are actively trained. Adjusting these parameters directly influences computational load and memory consumption. For the first parameter, we follow Meng et al. (2022) and Rao et al. (2021) by reducing the number of tokens processed, selectively removing redundant ones during the forward pass. For the second parameter, we freeze less critical layers, saving memory and preventing unnecessary updates to their weights during the backward pass (Figure 1). We highlight that the proposed method can be integrated into existing fine-tuning frameworks with minimal overhead. We provide an overview of ALaST in Figure 3. To implement the budget allocation, we first need a reliable method to estimate the importance of each layer.

#### 3.1 Estimating the importance of each layer

In the following, we explain how we assign a budget to each transformer layer. We assume that each fine-tuning step comprises a forward and a backward pass. We use  $i$  to indicate the current step and  $\text{CLS}_i^l$  to indicate the embedding of the class token at layer  $l$  for step  $i$ . Given a fine-tuning step  $i$ , we estimate the importance of each layer  $l$  and assign it a training budget  $b_l^i \in (0, 1)$ , representing the computational resources we can afford to spend on that layer. The budget should be high if the layer’s contribution to the final prediction is high, low otherwise. Notably, the budget must be computed *adaptively at each step*.

During the forward pass, the class token aggregates information from all other tokens and it is passed through the classification head. This token is crucial for capturing rich semantic information about the input, making it a reliable indicator for evaluating each layer’s contribution to the final prediction. The class token’s role in capturing essential features for downstream tasks has already been investigated in previous works, such as Raghu et al. (2021), which studied the correlation between the CLS token representation and each layer’s contribution to the final prediction. This correlation can be intuitively understood by noting that the class token, being the only one that is passed through the final classifier, must capture information about the whole input image (Liang et al. 2022; Raghu et al. 2021). As a result, layers that contribute less to updating the class token are less critical, and we assign them lower compute budgets without impacting overall performance.

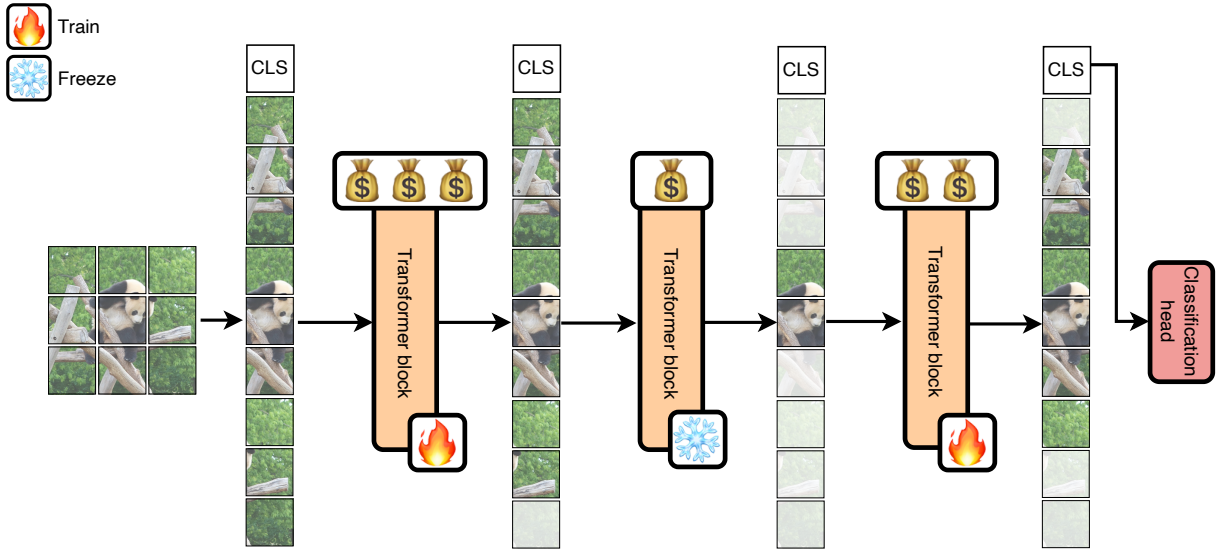


Figure 3: At each fine-tuning iteration, each layer is assigned a compute budget. Based on the budget, we allow more (high budget) or fewer (low budget) tokens to flow through the layer - greyed out tokens are excluded from computation. Additionally, we freeze layers with the lowest budgets to save computing resources and memory.

We now provide a more detailed explanation of how we estimate the appropriate budget for each layer based on this observation. At fine-tuning step  $i$ , layer  $l$  updates the class token according to:

$$\text{CLS}_l^i = \mathcal{F}^l(\text{CLS}_{l-1}^i) \quad (4)$$

where  $\text{CLS}_{l-1}^i$  is the class token representation coming from the previous layer,  $\mathcal{F}^l$  represents the function applied by layer  $l$ , and  $\text{CLS}_l^i$  is the updated class token representation. To capture the variations in the class token embedding, we define the class token delta at layer  $l$  and training step  $i$  as:

$$\Delta_l^i = (\text{CLS}_l^i - \text{CLS}_{l-1}^i)^2 \quad (5)$$

The class token delta quantifies the magnitude of the update performed by layer  $l$  on the class token’s residual stream. Finally, we use the variation in class token deltas across iterations to compute the training budget. At the next training iteration  $i + 1$ , we compute:

$$b_l^{i+1} = b_l^i + (\Delta_l^{i+1} - \Delta_l^i) \times \alpha \quad (6)$$

Here,  $b_l^i$  represents the budget from the previous training iteration, and  $\alpha$  is the budget learning rate, which we initialize to match the fine-tuning learning rate. We always initialize the budget to 1 for each layer, and clip it during fine-tuning to have a value between 0 and 1. By assigning a budget to each layer, we obtain a distribution of budgets  $\mathcal{D}_L^i$ , where  $L$  is the number of layers and  $i$  is the current training step. We provide an example of how compute budgets vary during fine-tuning in Figure 7. We then leverage this budget distribution to allocate resources appropriately across layers.

### 3.2 Applying the budget

Based on the distribution of budgets  $\mathcal{D}_L^i$ , we allocate our memory and FLOPs resources leveraging two degrees of

freedom: the number of processed tokens and the trainable layers. In the two following paragraphs, we explain how we select which tokens to discard and which layers to freeze.

**Adaptive Token selection** As pointed out in several works (Jain et al. 2024; Meng et al. 2022; Bolya et al. 2023) not all tokens carry equally valuable information for the task at hand. Given an input sequence  $T \in \mathcal{R}^{N \times E}$ , where  $N$  is the sequence length and  $E$  is the embedding dimension, we only allow  $b \cdot N$  tokens to flow to the next layer. Here,  $b \in [0, 1]$ , meaning that this approach selects  $b\%$  of the tokens from the input sequence. To determine which tokens to discard, we adopt a strategy similar to that of Liang et al. (2022). We rank the tokens based on their attention scores from the CLS token and retain only the top  $b \cdot N$  tokens.

This approach leverages the fact that tokens with higher attention scores are more influential in determining the class prediction, as we show in Figure 4, where we plot some attention maps with respect to the class token for DeiT-S. By retaining only the most important tokens - those that contribute significantly to the class token’s representation - we reduce computational overhead and memory usage while preserving the most relevant information for classification. Initially, we allowed unattended tokens to proceed to the next layer. However, analysis of attention score distributions revealed that tokens excluded at one layer remained excluded in subsequent layers. Consequently, we opted to discard the least attended tokens, preventing their progression to the next layer. This approach further reduced batch size and memory consumption without performance loss.

**Adaptive Layer Freezing** In addition to token selection, we also optimize resource allocation by freezing certain layers. Given a budget  $b$ , we freeze the less critical layers to conserve memory, which is crucial for efficient on-device

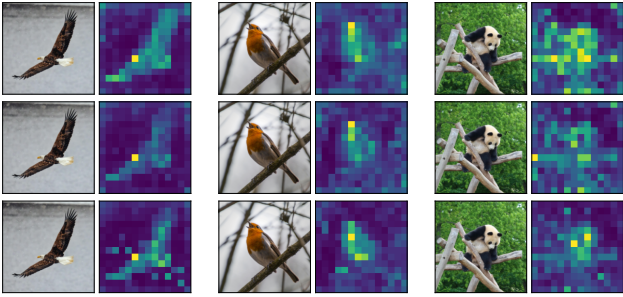


Figure 4: Attention of CLS token for different patches at layer 2,4,6 of DeiT-S (Touvron et al. 2021). Brighter patches have higher attention. CLS token’s attention captures semantically important patches.

training. By freezing these layers, we reduce the number of trainable parameters, thereby lowering memory consumption and improving computational efficiency. When a layer is frozen, we save the memory which is necessary to store the activations for the backpropagation. After determining the budget distribution  $\mathcal{D}_L^i$ , we sample layers  $\mathbf{x} \sim \mathcal{D}_L^i$  without replacement, ensuring that the same layer is not selected twice. We then train only the  $K$  layers with the highest budget allocation, and freeze the rest. The dual approach of token selection and layer freezing enables us to manage resources effectively and optimize the performance of our model within the constraints of the available device memory, by leveraging two different degrees of liberty.

## 4 Experimental Setup

We fine-tune our models on Flower-102 Nilsback and Zisserman, Cifar-100 Krizhevsky, Nair, and Hinton and the more challenging Food-101 Bossard, Guillaumin, and Van Gool dataset. We test a larger pre-trained Vision Transformer ViT-B (Dosovitskiy et al. 2021) along with the DeiT-S and DeiT-T (Touvron et al. 2021) models, that are smaller and more parameter efficient, thus more likely to be used in resource-constrained scenarios. We show the tested model architectures in Table 1. We download pre-trained weights from timm-models (Wightman 2019). In all the runs, we set  $K$  (number of trainable layers) to 9, but we show results for other values in Appendix B. We use mixed precision training (Micikevicius et al. 2018) for all our experiments to keep memory usage as small as possible and simulate a real-world on-device training. During training, we keep track of FLOPs (Floating Point Operations), memory load and wall-clock time. While memory and time are important metrics to assess practical performance and resource utilization, they can be partially influenced by hardware. Therefore, we also use FLOPs to provide a hardware-independent measure of computational complexity, enabling consistent cross-system comparisons. For reproducibility, we provide detailed descriptions of our experimental setup, including code, hyper-parameters, and training procedures in Appendix E.

Model	embedding	#heads	#layers	#params
DeiT-T	192	3	12	5M
DeiT-S	384	6	12	22M
ViT-B	768	12	12	86M

Table 1: Variants of tested ViT architectures.

## 5 Results & Analysis

We evaluate our method against a diverse array of baselines, including both traditional fine-tuning approaches and state-of-the-art techniques, including Low-Rank Adaptation (LoRA) (Hu et al. 2022), Token merging (Bolya et al. 2023) and Block Selective Reprogramming (Sarkar et al. 2024). Compared to standard fine-tuning procedures, ALaST achieves optimal performance at a fraction of the cost. While fine-tuning all layers typically results in high final accuracy, it comes at the expense of significantly more expensive training. In Figure 5, we demonstrate the normalized gains our method achieves compared to full fine-tuning. With ALaST, we observe only a minimal reduction in accuracy while using just 60% of the FLOPs, 50% of the memory, and 80% of the fine-tuning wall-clock time relative to the full fine-tuning baseline, without adding any additional parameters. An alternative to full fine-tuning is training only the classification head, which is computationally and memory efficient since only the final linear layer is updated via back-propagation. However, this approach typically results in substantially lower final accuracy. ALaST strikes a balance between these two extremes, maintaining low memory usage and training FLOPs, while losing only minimal accuracy compared to full fine-tuning. A more detailed comparison can be found in Figure 6. In low-resource scenarios, it is critical not only to reduce the total resources consumed during fine-tuning but also to manage the distribution of these resources throughout the training process. Often, training until full convergence is not feasible, making the initial “speed” of convergence particularly important. In other words, a method that requires fewer FLOPs but converges slowly is impractical for such constrained environ-

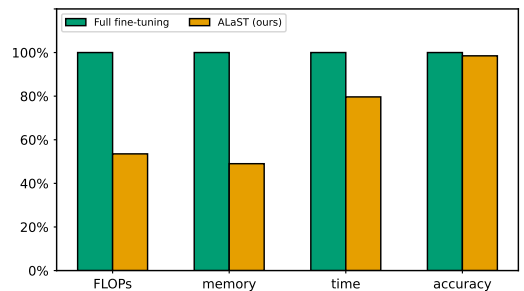


Figure 5: Normalized improvement when fine-tuning with ALaST with respect to full fine-tuning for FLOPs, Memory, wall-clock time and accuracy. On average, we achieve similar accuracy, with 60% FLOPs, 50% memory and 80% time. We average the results on all the considered datasets for DeiT-S.

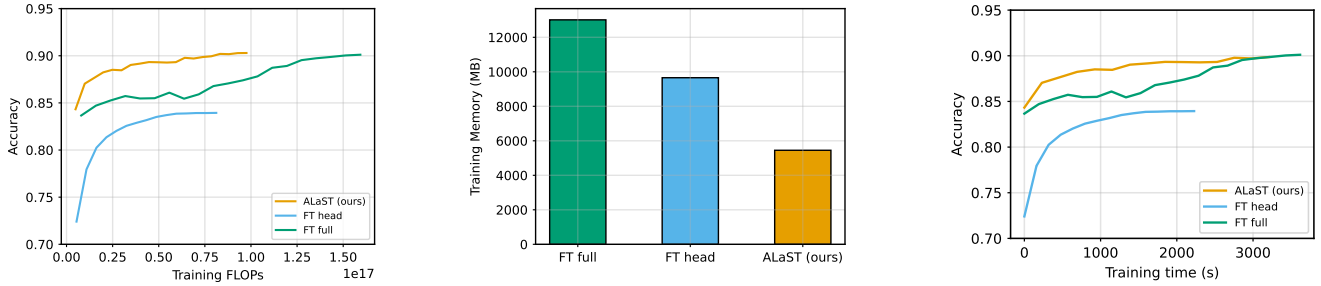


Figure 6: Comparison for ViT-B on a fixed data budget of 20 epochs for Food-101. Our method converges with fewer FLOPs (left), lower memory (center) and shorter time (right), with respect to fine-tuning all layers (FT full) and only head (FT head).

ments. As shown in Figure 6, thanks to its dynamic compute budget allocation, ALaST converges to higher accuracy in less time and with fewer FLOPs, making it well-suited for resource-constrained scenarios.

**Comparison to other methods** In Table 2 and Table 3 we provide more detailed results on Food-101 and Cifar-100, and report results on Flower-102 in Appendix A to conserve space. For each method, we track training FLOPs, peak training memory, and wall-clock time. We compare our approach to six different fine-tuning baselines. Token Merging (ToMe) (Bolya et al. 2023) merges  $r$  tokens at each transformer layer, using an optimal  $r$  as determined by hyperparameter search. For Block Selective Reprogramming (BSR), we follow the methodology proposed in (Sarkar et al. 2024) and select the three most influential blocks, while simultaneously discarding tokens. Another baseline involves identifying the three most influential blocks through exploration and training only those blocks (FT top-3). Finally, we also include a comparison with the popular LoRA method (Hu et al. 2022). A key distinction of our method is that, unlike ToMe, FT top-3, and BSR, it *adaptively* learns which layers are most important, eliminating the need for extensive experimentation to identify the crucial layers in advance. Compared to LoRA, our method does not add any parameters to the model.

While ToMe is effective at minimizing memory consumption, it struggles to achieve high accuracy, particularly with larger models. This limitation likely stems from the fixed  $r$  schedule, which is predetermined and not adjusted during training, causing some layers to "starve" at different stages of fine-tuning. In contrast, ALaST dynamically allocates computational resources to the most critical layers, leading to a more efficient use of the computational budget. BSR, on the other hand, preselects which layers to freeze and discards tokens accordingly. This preselection results in a suboptimal combination of frozen layers, leading to lower accuracy and higher memory usage during fine-tuning compared to our method. We observe that LoRA's accuracy degrades significantly with smaller DeiT-T and DeiT-S models. This is likely due to the reduced representational capacity of smaller models, that makes it hard to adjust to a new distribution only leveraging LoRA's additional parameters, leading to relatively lower performance improvements. On

larger ViT-B, LoRA seems to achieve a similar performance to our method at the cost of a higher memory load needed to store all the activations. Because our method is orthogonal to PEFT strategies in general, we also experiment with integrating it with LoRA in Appendix C.

**Layer Budgets across Fine-tuning** Budget assignment is dynamic and happens at each fine-tuning iteration. For DeiT-S and ViT-B, higher compute budgets are usually allocated to the first layers already in the initial part of the fine-tuning, as we show in Figure 7. Interestingly, for the first two layers, the method allocates high budgets across the entire fine-tuning, while for central layers the budget usually decreases significantly or exhibits a higher variance. For DeiT-T, we observe a different pattern, where first and last layers are allocated higher budgets, while central ones are often neglected. We show more plots and results analyzing budget allocation in Appendix D.

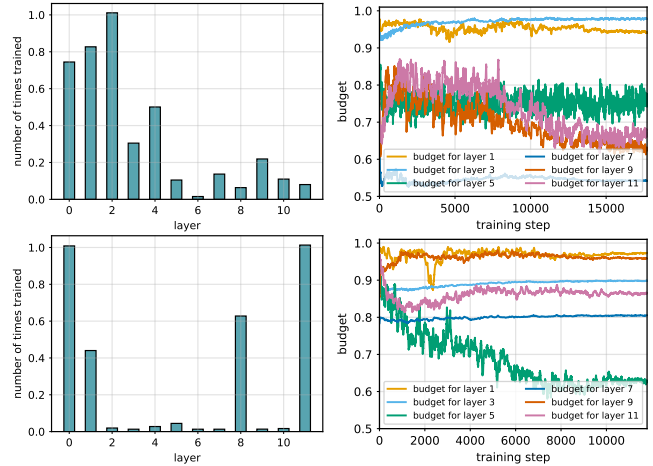


Figure 7: Compute budget allocation during fine-tuning of DeiT-S (top) and DeiT-T (bottom) on Food-101. Left: absolute training frequency per layer. Right: budget variation across training. Additional plots for different models and datasets are in Appendix D

Table 2: Fine-tuning DeiT-T, DeiT-S and ViT-B on Food-101. Proposed method results and best results in bold.

Model	Deit-t-16				Deit-s-16				ViT-B			
	Compute (PFLOPs)	Memory (MB)	Time (min)	Accuracy	Compute (PFLOPs)	Memory (MB)	Time (min)	Accuracy	Compute (PFLOPs)	Memory (MB)	Time (min)	Accuracy (top-1)
FT head	7.5	<b>2389</b>	<b>13.44</b>	0.59	10.5	4751	<b>18.36</b>	0.70	<b>80</b>	9657	<b>35.47</b>	0.83
FT full	11.2	3267	24.13	<b>0.83</b>	30.2	7186	33.08	<b>0.86</b>	150	13012	64.37	<b>0.90</b>
FT top-3	9.6	2525	15.17	0.8	22.8	5202	20.40	0.84	120	7096	39.45	0.90
ToME [1]	7.5	2983	18.06	0.82	<b>10.0</b>	<b>2134</b>	25.05	0.80	153	<b>4493</b>	48.42	<b>0.88</b>
BSR [34]	8.5	2500	14.30	0.80	12.3	3520	19.38	0.83	117	6900	37.46	0.88
LoRA [13]	8.2	2620	26.44	0.78	22.5	5060	35.12	0.83	109	11823	48.35	0.89
ALaST (ours)	<b>5.1</b>	<b>1724</b>	<b>18.0</b>	<b>0.81</b>	<b>14.5</b>	<b>4190</b>	<b>25.05</b>	<b>0.86</b>	<b>107</b>	<b>5451</b>	<b>48.42</b>	<b>0.90</b>

Table 3: Fine-tuning DeiT-T, DeiT-S and ViT-B on Cifar-100. Proposed method results and best results in bold.

Model	Deit-t-16				Deit-s-16				ViT-B			
	Compute (PFLOPs)	Memory (MB)	Time (min)	Accuracy	Compute (PFLOPs)	Memory (MB)	Time (min)	Accuracy	Compute (PFLOPs)	Memory (MB)	Time (min)	Accuracy
FT head	<b>5.0</b>	<b>2389</b>	<b>8.18</b>	0.66	<b>18.4</b>	4751	<b>11.34</b>	0.75	<b>70</b>	9657	<b>22.40</b>	0.84
FT full	7.8	3267	14.14	<b>0.84</b>	27.1	7186	20.14	<b>0.88</b>	90	13012	40.34	0.90
FT top-3	6.3	2525	9.13	0.82	21.0	5202	12.51	0.87	80	7096	24.11	<b>0.92</b>
ToME [1]	7.1	2983	11.32	<b>0.84</b>	26.7	<b>3122</b>	35.23	0.88	75	<b>4493</b>	30.29	0.86
BSR [34]	6.0	3052	8.45	0.82	13.0	3500	12.13	0.87	79	6900	23.30	0.91
LoRA [13]	5.5	2643	15.10	0.81	22.3	5060	32	0.85	80	11823	32.10	0.90
ALaST (ours)	<b>5.0</b>	<b>2397</b>	<b>11.32</b>	<b>0.83</b>	<b>15.5</b>	<b>3613</b>	<b>15.05</b>	<b>0.87</b>	<b>70</b>	<b>5341</b>	<b>29.30</b>	<b>0.90</b>

## 6 Related Works

### 6.1 Parameter Efficient Fine-Tuning

In the last years, the field of parameter efficient fine-tuning (PEFT) has seen increased interest. One of the first approaches in PEFT was the use of adapters, [Houlsby et al.](#), that insert and fine-tune small neural network modules into each layer of a pre-trained model. Prefix-tuning [Li and Liang](#) and prompt-tuning [Lester, Al-Rfou, and Constant](#) learn soft prompts that are added to the input tokens. Perhaps the most popular PEFT approach is LoRA (Low-Rank Adaptation), proposed in ([Hu et al. 2022](#)), that reduces the number of additional parameters that need to be fine-tuned by decomposing the weight updates into a product of two low-rank matrices. Most of the PEFT methods were introduced for fine-tuning large language models, and subsequently applied to computer vision with varying degrees of success ([Xin et al. 2024](#)). Typically, these approaches emphasize optimizing the number of additional parameters rather than FLOPs or training time. However, parameters memory is only a fraction of the memory used during training. Unlike PEFT, ALaST does not add any parameters, and also reduces FLOPs and memory. Additionally, ALaST can be combined with LoRA, as we show in Appendix C.

### 6.2 On-device Training

Our work is perhaps most similar to those papers that optimize resources for on-device training. Among these, ([Cai et al. 2020](#)) was the first to highlight that memory is a major bottleneck in CNN training and devise a way to reduce memory load. Along the same line, some approaches proposed to recompute activations for a subset of the layers to reduce memory consumption ([Chen et al. 2016](#); [Gruslys et al. 2016](#)). While this strategy can be useful for low memory budgets, it sacrifices the compute (FLOPs), and is not suitable for devices with limited computational resources.

Recently, [Sarkar et al. \(2024\)](#); [Samragh et al. \(2023\)](#) explored smart initialization by identifying the best subset of layers to fine-tune. [Sarkar et al. \(2024\)](#) identifies the most important layers and discards redundant tokens during fine-tuning. [Samragh et al. \(2023\)](#) uses the relative magnitude of outputs to estimate the importance of different blocks and initialize a smaller model from a larger one. Unlike these methods, ALaST learns the importance of individual layers during fine-tuning and therefore does not need extensive research of which layers to train in advance.

### 6.3 Efficient Transformers

A substantial body of research has focused on enhancing the efficiency of ViTs, particularly during the inference phase. For example, ([Rao et al. 2021](#); [Meng et al. 2022](#)) proposed token halting strategies that select the most important tokens at runtime and speed up inference. [Touvron et al. \(2021\)](#) employed distillation from CNNs to maintain model accuracy while reducing the number of parameters and FLOPs. [Lin et al. \(2022\)](#) introduced a quantized version of the Vision Transformer to decrease model inference complexity. More recently, [Wójcik et al. \(2023\)](#) proposed to control the computational load by activating sub-modules of the transformer, based on input difficulty. In contrast to these methods, we do not focus on inference, but address the challenge of fine-tuning available foundation models when resources are limited.

## 7 Conclusions

We introduced ALaST, a simple and effective method to fine-tune ViTs in low-resource scenarios, saving computational budget, memory load and training time, with minimal modifications to the training pipeline. Although we test ALaST on ViTs, its principles are generalizable to other transformer-based architectures, which we plan to explore in future work.

## Acknowledgements

This work has been supported by the SNS JU project 6G-GOALS under the EU's Horizon program Grant Agreement No 101139232, by Sapienza grant RG123188B3EF6A80 (CENTS), and by European Union under the Italian National Recovery and Resilience Plan of NextGenerationEU, partnership on Telecommunications of the Future (PE00000001 - program RESTART)

## References

- Bolya, D.; Fu, C.-Y.; Dai, X.; Zhang, P.; Feichtenhofer, C.; and Hoffman, J. 2023. Token Merging: Your ViT but Faster. In *International Conference on Learning Representations*.
- Bossard, L.; Guillaumin, M.; and Van Gool, L. 2014. Food-101 – Mining Discriminative Components with Random Forests. In *European Conference on Computer Vision*.
- Cai, H.; Gan, C.; and Han, S. 2022. Efficientvit: Enhanced linear attention for high-resolution low-computation visual recognition. *arXiv preprint arXiv:2205.14756*.
- Cai, H.; Gan, C.; Zhu, L.; and Han, S. 2020. TinyTL: Reduce Memory, Not Parameters for Efficient On-Device Learning. In Larochelle, H.; Ranzato, M.; Hadsell, R.; Balcan, M.; and Lin, H., eds., *Advances in Neural Information Processing Systems*, volume 33, 11285–11297. Curran Associates, Inc.
- Calvanese Strinati, E.; Di Lorenzo, P.; Sciancalepore, V.; Aijaz, A.; Kountouris, M.; Gündüz, D.; Popovski, P.; Sana, M.; Stavrou, P. A.; and et al. 2024. Goal-oriented and semantic communication in 6G AI-native networks: The 6G-GOALS approach. In IEEE, ed., *EuCNC & 6G Summit 2024, European Conference on Networks and Communications (EuCNC) and the 6G Summit, 3-6 June 2024, Antwerp, Belgium*. Antwerp.
- Chen, T.; Xu, B.; Zhang, C.; and Guestrin, C. 2016. Training Deep Nets with Sublinear Memory Cost. *arXiv:1604.06174*.
- Dodge, J.; Ilharco, G.; Schwartz, R.; Farhadi, A.; Hajishirzi, H.; and Smith, N. 2020. Fine-tuning pretrained language models: Weight initializations, data orders, and early stopping. *arXiv preprint arXiv:2002.06305*.
- Dosovitskiy, A.; Beyer, L.; Kolesnikov, A.; Weissenborn, D.; Zhai, X.; Unterthiner, T.; Dehghani, M.; Minderer, M.; Heigold, G.; Gelly, S.; Uszkoreit, J.; and Houlsby, N. 2021. An Image is Worth 16x16 Words: Transformers for Image Recognition at Scale. In *International Conference on Learning Representations*.
- Elhage, N.; Nanda, N.; Olsson, C.; Henighan, T.; Joseph, N.; Mann, B.; Askell, A.; Bai, Y.; Chen, A.; Conerly, T.; DasSarma, N.; Drain, D.; Ganguli, D.; Hatfield-Dodds, Z.; Hernandez, D.; Jones, A.; Kernion, J.; Lovitt, L.; Ndousse, K.; Amodei, D.; Brown, T.; Clark, J.; Kaplan, J.; McCandlish, S.; and Olah, C. 2021. A Mathematical Framework for Transformer Circuits. *Transformer Circuits Thread*. <https://transformer-circuits.pub/2021/framework/index.html>.
- Gromov, A.; Tirumala, K.; Shapourian, H.; Glorioso, P.; and Roberts, D. A. 2024. The Unreasonable Ineffectiveness of the Deeper Layers. *arXiv:2403.17887*.
- Gruslys, A.; Munos, R.; Danihelka, I.; Lanctot, M.; and Graves, A. 2016. Memory-efficient backpropagation through time. In *Proceedings of the 30th International Conference on Neural Information Processing Systems, NIPS'16*, 4132–4140. Red Hook, NY, USA: Curran Associates Inc. ISBN 9781510838819.
- Houlsby, N.; Giurgiu, A.; Jastrzebski, S.; Morrone, B.; De Laroussilhe, Q.; Gesmundo, A.; Attariyan, M.; and Gelly, S. 2019. Parameter-Efficient Transfer Learning for NLP. In Chaudhuri, K.; and Salakhutdinov, R., eds., *Proceedings of the 36th International Conference on Machine Learning*, volume 97 of *Proceedings of Machine Learning Research*, 2790–2799. PMLR.
- Hu, E. J.; yelong shen; Wallis, P.; Allen-Zhu, Z.; Li, Y.; Wang, S.; Wang, L.; and Chen, W. 2022. LoRA: Low-Rank Adaptation of Large Language Models. In *International Conference on Learning Representations*.
- Jain, G.; Hegde, N.; Kusupati, A.; Nagrani, A.; Buch, S.; Jain, P.; Arnab, A.; and Paul, S. 2024. Mixture of Nested Experts: Adaptive Processing of Visual Tokens. <https://arxiv.org/abs/2407.19985>.
- Kingma, D.; and Ba, J. 2015. Adam: A Method for Stochastic Optimization. In *International Conference on Learning Representations (ICLR)*. San Diego, CA, USA.
- Krizhevsky, A.; Nair, V.; and Hinton, G. 2009. CIFAR-100 (Canadian Institute for Advanced Research).
- Laskaridis, S.; Venieris, S. I.; Almeida, M.; Leontiadis, I.; and Lane, N. D. 2020. SPINN: synergistic progressive inference of neural networks over device and cloud. In *Proceedings of the 26th Annual International Conference on Mobile Computing and Networking, MobiCom '20*. Association for Computing Machinery. ISBN 9781450370851.
- Lester, B.; Al-Rfou, R.; and Constant, N. 2021. The Power of Scale for Parameter-Efficient Prompt Tuning. In Moens, M.-F.; Huang, X.; Specia, L.; and Yih, S. W.-t., eds., *Proceedings of the 2021 Conference on Empirical Methods in Natural Language Processing*, 3045–3059. Online and Punta Cana, Dominican Republic: Association for Computational Linguistics.
- Li, X. L.; and Liang, P. 2021. Prefix-Tuning: Optimizing Continuous Prompts for Generation. In Zong, C.; Xia, F.; Li, W.; and Navigli, R., eds., *Proceedings of the 59th Annual Meeting of the Association for Computational Linguistics and the 11th International Joint Conference on Natural Language Processing (Volume 1: Long Papers)*, 4582–4597. Association for Computational Linguistics.
- Liang, Y.; GE, C.; Tong, Z.; Song, Y.; Wang, J.; and Xie, P. 2022. EViT: Expediting Vision Transformers via Token Reorganizations. In *International Conference on Learning Representations*.
- Lin, Y.; Zhang, T.; Sun, P.; Li, Z.; and Zhou, S. 2022. FQ-ViT: Post-Training Quantization for Fully Quantized Vision Transformer. In *Proceedings of the Thirty-First International Joint Conference on Artificial Intelligence, IJCAI-22*, 1173–1179.
- Liu, H.; Li, C.; Wu, Q.; and Lee, Y. J. 2023. Visual Instruction Tuning. In *NeurIPS*.



- Matthias Minderer, A. G. e. a. 2022. Simple Open-Vocabulary Object Detection with Vision Transformers. *arXiv preprint arXiv:2205.06230*.
- Mehta, S.; and Rastegari, M. 2022. MobileViT: Lightweight, General-purpose, and Mobile-friendly Vision Transformer. In *International Conference on Learning Representations*.
- Meng, L.; Li, H.; Chen, B.-C.; Lan, S.; Wu, Z.; Jiang, Y.-G.; and Lim, S.-N. 2022. Advit: Adaptive vision transformers for efficient image recognition. In *Proceedings of the IEEE/CVF Conference on Computer Vision and Pattern Recognition*, 12309–12318.
- Micikevicius, P.; Narang, S.; Alben, J.; Diamos, G.; Elsen, E.; Garcia, D.; Ginsburg, B.; Houston, M.; Kuchaiev, O.; Venkatesh, G.; and Wu, H. 2018. Mixed Precision Training. In *International Conference on Learning Representations*.
- Nilsback, M.-E.; and Zisserman, A. 2008. Automated Flower Classification over a Large Number of Classes. In *Indian Conference on Computer Vision, Graphics and Image Processing*.
- Paszke, A.; Gross, S.; Chintala, S.; Chanan, G.; Yang, E.; DeVito, Z.; Lin, Z.; Desmaison, A.; Antiga, L.; and Lerer, A. 2017. Automatic differentiation in PyTorch. In *NIPS-W*.
- Radford, A.; Kim, J. W.; Hallacy, C.; Ramesh, A.; Goh, G.; Agarwal, S.; Sastry, G.; Askell, A.; Mishkin, P.; Clark, J.; Krueger, G.; and Sutskever, I. 2021. Learning Transferable Visual Models From Natural Language Supervision. In Meila, M.; and Zhang, T., eds., *Proceedings of the 38th International Conference on Machine Learning*, volume 139 of *Proceedings of Machine Learning Research*, 8748–8763. PMLR.
- Raghu, M.; Unterthiner, T.; Kornblith, S.; Zhang, C.; and Dosovitskiy, A. 2021. Do Vision Transformers See Like Convolutional Neural Networks? In Beygelzimer, A.; Dauphin, Y.; Liang, P.; and Vaughan, J. W., eds., *Advances in Neural Information Processing Systems*.
- Rao, Y.; Zhao, W.; Liu, B.; Lu, J.; Zhou, J.; and Hsieh, C.-J. 2021. Dynamicvit: Efficient vision transformers with dynamic token sparsification. *Advances in neural information processing systems*, 34: 13937–13949.
- Russakovsky, O.; Deng, J.; Su, H.; Krause, J.; Satheesh, S.; Ma, S.; Huang, Z.; Karpathy, A.; Khosla, A.; Bernstein, M.; Berg, A. C.; and Fei-Fei, L. 2015. ImageNet Large Scale Visual Recognition Challenge. *International Journal of Computer Vision (IJCV)*, 115(3): 211–252.
- Samragh, M.; Farajtabar, M.; Mehta, S.; Vemulapalli, R.; Faghri, F.; Naik, D.; Tuzel, O.; and Rastegari, M. 2023. Weight subcloning: direct initialization of transformers using larger pretrained ones.
- Sarkar, S.; Kundu, S.; Zheng, K.; and Beerel, P. A. 2024. Block Selective Reprogramming for On-device Training of Vision Transformers. *arXiv:2405.10951*.
- Touvron, H.; Cord, M.; Douze, M.; Massa, F.; Sablayrolles, A.; and Jegou, H. 2021. Training data-efficient image transformers with distillation through attention. In *International Conference on Machine Learning*, volume 139, 10347–10357.
- Wightman, R. 2019. PyTorch Image Models. <https://github.com/rwightman/pytorch-image-models>.
- Wójcik, B.; Devoto, A.; Pustelnik, K.; Minervini, P.; and Scardapane, S. 2023. Adaptive Computation Modules: Granular Conditional Computation For Efficient Inference.
- Xin, Y.; Luo, S.; Zhou, H.; Du, J.; Liu, X.; Fan, Y.; Li, Q.; and Du, Y. 2024. Parameter-Efficient Fine-Tuning for Pre-Trained Vision Models: A Survey. *arXiv:2402.02242*.
- Yin, H.; Vahdat, A.; Alvarez, J. M.; Mallya, A.; Kautz, J.; and Molchanov, P. 2022. A-vit: Adaptive tokens for efficient vision transformer. In *Proceedings of the IEEE/CVF Conference on Computer Vision and Pattern Recognition*, 10809–10818.
- Zhang, C.; Bengio, S.; and Singer, Y. 2022. Are All Layers Created Equal?

## A Additional Results

We show additional results on the Flower-102 dataset in table Table 7. Flower-102 is the smallest dataset that we use for our experiments.

## B Number of trainable blocks

At each iteration, we select  $K$  transformer layers for fine-tuning. We showed experiments with  $K = 9$ . Here we report results for different values of  $K$ . In Figure 8 we show the accuracy and FLOPs trade-off for different values of  $K$ . We see that increasing the number of trainable layers leads to better performance in general. The improvement becomes smaller when  $K$  is greater than 8. We report detailed results in Table 4.

## C Combination with PEFT

As we showed in Table 3 and Table 2, LoRA performs rather poorly when applied to smaller models, while ALaST converges faster and to higher accuracy. On larger ViT-B, on the other hand, LoRA achieves similar accuracy to our method, at a higher memory cost to store the activations for all layers. Because the two methods are orthogonal, we integrate them and test LoRA + ALaST on ViT-B.

In order to combine LoRA with ALaST, we apply the budget schedule to LoRA’s additional parameters and keep the transformer layers frozen, except for the classification head. We report results for Cifar-100 and Food-101 in Table 5 and Table 6, respectively. By intergrating LoRA with ALaST, we further reduce the memory footprint, while still achieving accuracy comparable to baseline.

## D Compute Budget Allocation

In Figure 9 we show the total number of times each layer is chosen during fine-tuning. We see that for DeiT-S and ViT-B the compute budget is more evenly distributed across layers, and initial layers are usually picked more frequently. In the smaller DeiT-T, on the other hand, the budget is allocated mainly to initial and last layers, and the distribution

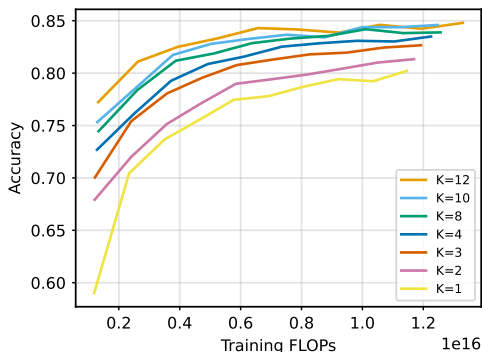


Figure 8: Accuracy vs FLOPs trade-off during fine-tuning, with different number of trainable layers for DeiT-S on Food-101.

results more peaked. In Figure 10 we show the budget assignment during fine-tuning. We observe that central layers usually exhibit a higher variance of assigned compute budget. In DeiT-S and ViT-B we observe a pattern where deeper layers are assigned high budget in the first iterations, and the budget is then decreased along fine-tuning. For the initial layers on the other hand, the budget is usually constantly high across the entire fine-tuning.

## E Implementation details

In the following, we provide details on the implementation and fine-tuning hyper-parameters. We fine-tune the three models using Adam optimizer (Kingma and Ba 2015) with a batch size of 128. After an initial grid search, we set the learning rate to 0.0001 for all methods but LoRA, where we found 0.001 to be more effective. We use two random augmentations picked between horizontal or vertical flipping and random cropping for all datasets and runs. All images are resized to  $224 \times 224$ , that is the required input size for the pretrained models. We download the weights of the models (pre-trained on ImageNet (Russakovsky et al. 2015)) from Timm Image models (Wightman 2019). During fine-tuning we keep track of FLOPs, peak memory and training time on an NVidia RTX4090 GPU. To measure FLOPs and memory load, we use PyTorch MACs counter and memory allocation tools (Paszke et al. 2017). Finally, we provide the Python code used for experiments.

Table 4: Different values for the number of trainable blocks at each iteration,  $K$ .

$K$	Compute (PFLOPs)	Memory (MB)	Time (min)	Accuracy
1	11.6	3125	20	0.81
2	11.9	3211	21.30	0.83
3	12.0	3297	22.20	0.84
4	12.4	3383	23.50	0.85
8	13.0	3888	23.10	0.86
10	15.5	4000	24.10	0.86
12	15.8	4137	25.10	0.86

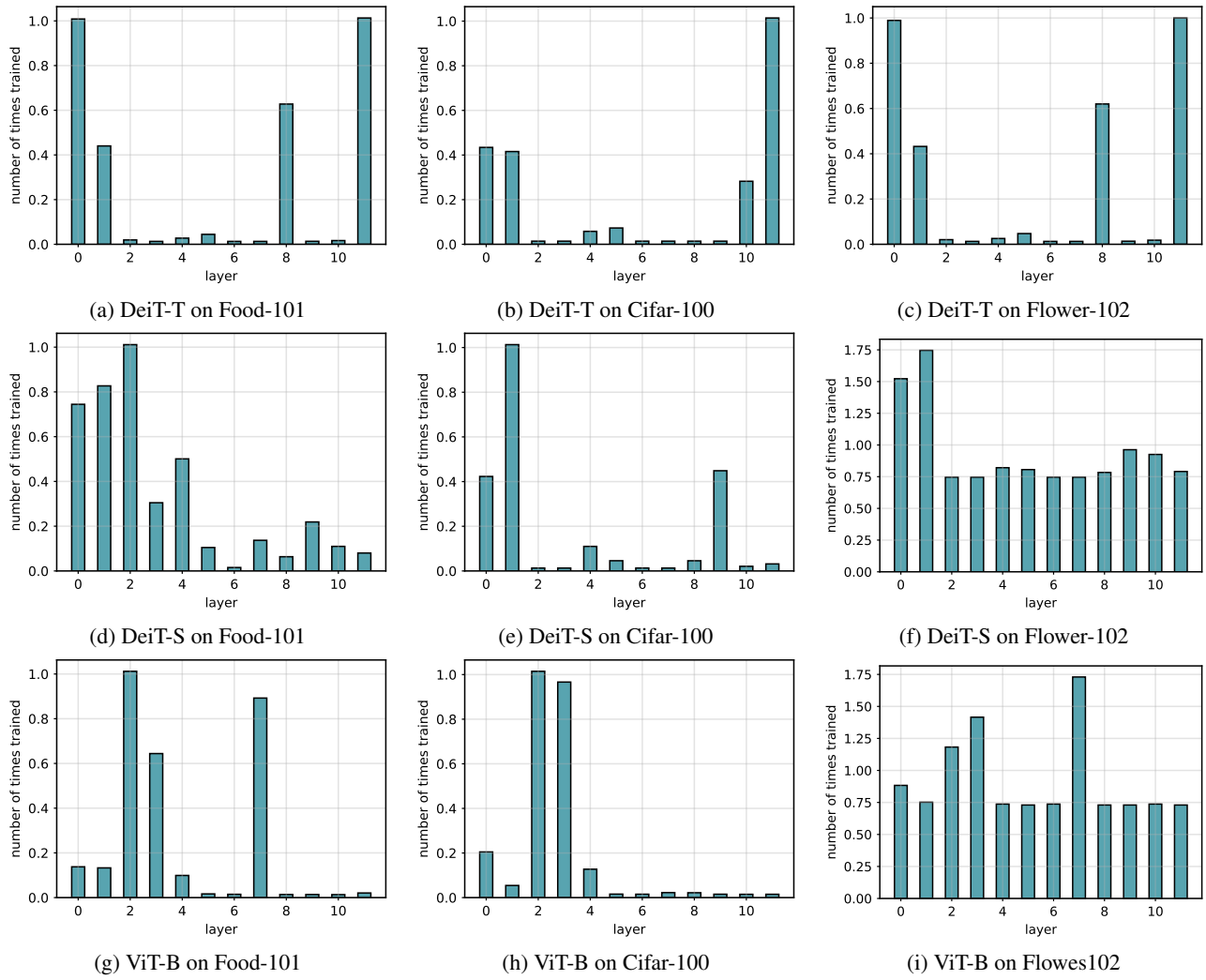


Figure 9: Final assignment on budgets for training on different datasets and models.

Table 5: Combining LoRA + ALaST for fine-tuning ViT-B on Cifar-100 dataset.

Method	Compute (PFLOPs)	Memory (MB)	Time (min)	Accuracy
FT full	90	13012	40.34	0.90
LoRA	80	11823	32.10	0.90
ALaST	70	5341	29.30	0.90
LoRA + ALaST	<b>50</b>	<b>4243</b>	21.20	<b>0.89</b>

Table 6: Combining LoRA + ALaST for fine-tuning ViT-B on Food-101 dataset

Method	Compute (PFLOPs)	Memory (MB)	Time (min)	Accuracy
FT full	150	13012	64.37	<b>0.90</b>
LoRA	109	11823	48.35	0.89
ALaST	107	5451	48.42	0.90
LoRA + ALaST	<b>95</b>	<b>4243</b>	41.00	<b>0.90</b>

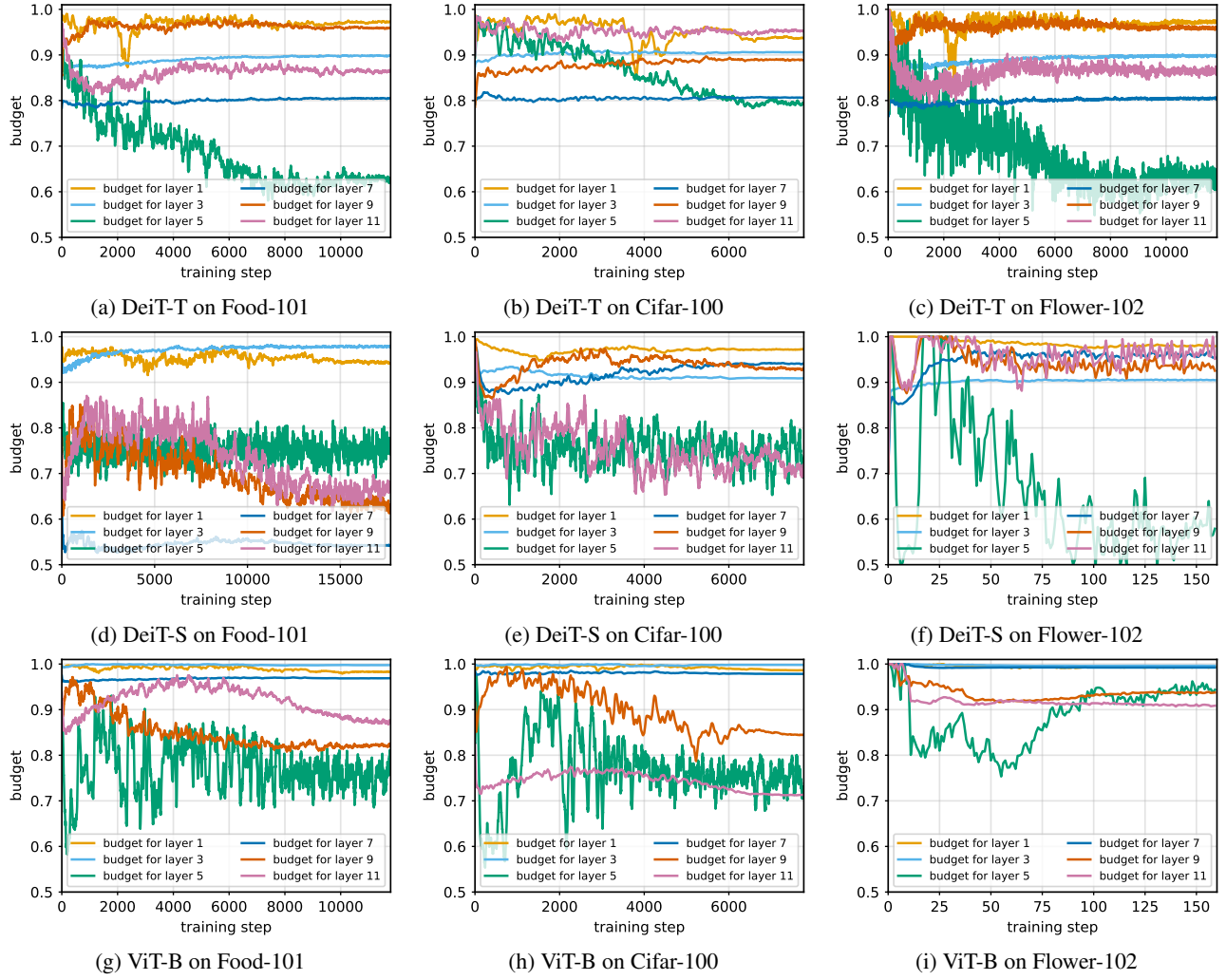


Figure 10: Compute budget assignment during fine-tuning.

Table 7: Comparison of Fine-tuning DeiT-T DeiT-S and ViT-B on Flower-102 dataset.

Model	DeiT-t-16				DeiT-s-16				ViT-B			
	Compute (PFLOPs)	Memory (MB)	Time (min)	Accuracy	Compute (PFLOPs)	Memory (MB)	Time (min)	Accuracy	Compute (PFLOPs)	Memory (MB)	Time (min)	Accuracy
FT head	0.12	2389	<b>1.11</b>	0.51	<b>0.3</b>	4751	1.5	0.54	<b>1.0</b>	9657	<b>3.58</b>	0.73
FT full	0.14	3267	2.12	0.72	0.5	7186	2.4	<b>0.89</b>	1.5	13012	7.18	<b>0.97</b>
FT top-3	0.12	2525	1.19	0.55	0.4	5202	1.2	0.77	1.2	7096	4.25	0.90
ToME [1]	0.13	2983	1.39	<b>0.88</b>	0.5	2134	3.0	0.88	1.3	<b>4493</b>	5.31	0.95
BSR [34]	<b>0.11</b>	<b>2000</b>	1.15	0.73	0.39	<b>3520</b>	<b>1.1</b>	0.76	<b>1.0</b>	6900	4.12	0.90
LoRA [13]	<b>0.11</b>	2400	2.19	0.56	0.5	7256	2.5	0.71	<b>1.0</b>	11823	7.44	<b>0.97</b>
ALaST (ours)	<b>0.8</b>	<b>3820</b>	<b>1.39</b>	<b>0.79</b>	<b>0.3</b>	<b>3523</b>	<b>2.2</b>	<b>0.9</b>	<b>1.5</b>	<b>5341</b>	<b>5.31</b>	<b>0.97</b>